Clustering, diffusion and evolution of COVID19 infections during lock-down

Wouter Bos, Jean-Pierre Bertoglio, and Louis Gostiaux
Univ Lyon, École Centrale de Lyon, INSA Lyon, Université Claude Bernard Lyon 1, CNRS, Laboratoire de Mécanique des Fluides et d'Acoustique, UMR 5509, 36 Avenue Guy de Collongue, F-69134, ECULLY, France

Epidemics such as the spreading of COVID19-virus are highly non linear, and therefore difficult to predict. In the present pandemy as time evolves, it appears more and more clearly that a clustered dynamics is a key element of description. This means that the disease rapidly evolves within spatially localized networks, that diffuse and eventually create new clusters. We improve upon the simplest possible compartmental model, the SIR model, by adding an additional compartment associated with the clustered individuals. The so-obtained SBIR model compares satisfactorily with results on the pandemic propagation in a number of European countries, during and immediately after lock-down. Especially, the decay exponent of the number of new cases after the first peak of the epidemic, is observed to be very similar for countries in which a strict lock-down is applied. We derive an analytical expression for the value of this exponent, relating it to the initial exponential growth phase of the epidemic and to the time-scale of cluster-diffusion.

I. LOCK-DOWN AND MODELING OF THE COVID19 EPIDEMIC

Since the beginning of the COVID19 epidemic in december 2019, many countries have chosen for severe restrictions on mobility and transport. It has become a controversial question in public debate whether these decisions were necessary and inevitable, and whether the lock-down was maintained for an unnecessary long period or, on the contrary was relaxed too soon in an unsafe way. In order to evaluate retrospectively such decisions, and to anticipate similar measures in the future, an in-depth understanding of epidemic propagation is needed. In the present investigation we focus on the seemingly universal way in which the COVID19 disease is controlled by lock-down.

Indeed, in a number of countries in which lock-down was applied, the number of new infections decays exponentially after the peak of the epidemic with a very similar time-scale (see Fig. 3). In the present investigation we shed light on the role of the finite size of spatially localized clusters on this phenomenon, by improving upon a simple paradigm model, the classical SIR model, and by assessing the resulting SBIR model against realistic data.

The SIR model in its simplest form contains three compartments, corresponding to susceptible, infected and recovered individuals, and the dynamics are governed by two model parameters α (recovery rate) and β (infection rate). A wide variety of SIR modifications have seen the light since its original formulation [1]. Many of them propose additional compartments (SEIR, others), nonlinear incidence rates [2], non-constant model coefficients (cite colleagues on covid from Lyon, Montpellier, Alizon, Roy, Derrode, Pillot). An overview of these models is beyond the scope of the present work and we refer to the review articles on the subject [3, 4].

In a large number of these epidemiologic studies using compartmental models, the dynamics are extremely sensitive on the temporal variations of the model parameters, and saturation of the epidemic at a realistic level is only obtained if the main parameters, such as the infection rate (or growth factor $R_0 = \beta/\alpha$) are changed during the analysis. We show that even using constant coefficients, saturation of the epidemic is obtained when the local nature of interactions within clusters is taken into account. Indeed, perhaps the largest known flaw of the SIR model is the assumption of well mixedness. In reality, not all individuals are in contact with all others, which is tacitly assumed by assimilating all susceptible individuals into one single compartment. The spatial structure of the epidemic is thereby ignored. An approach to overcome this weakness is to add spatial structure to the system by using either networks, self-propelled interacting agents, nested or coupled local SIR-type models [5] or diffusion equations (e.g. [6–8]). Such modifications change the level of complexity of the model considerably requiring either the solution of a two-dimensional reaction-diffusion problem, tracking a large number of propelled particles, or the solution of integro-differential equations. We refer to [9] for a discussion of the differences between agent-based and compartmental models.

The model we are introducing in the present work uses a two-scale approach: either individuals are far enough away from the individuals not to be in contact, or they pertain to a cluster of individuals in contact with the infected. This approach allows to take into account spatial structuring at the lowest level of complexity, i.e., by adding one single B-compartment, sub-dividing the group of susceptibles into those in a Blob, in contact with the infected, and S, those who are (spatially) distant. We will show, by comparison with data for a variety of European countries, that this model reproduces the exponential decay of the number of newly infected after its peak-value, with a correct exponent.

In the following we will first present the SBIR model and its difference with the classical SIR approach (section II). We will analytically determine the exponential decay time-scale for the SIR model with and without cross-immunity, as well as for the SBIR model. Finally we

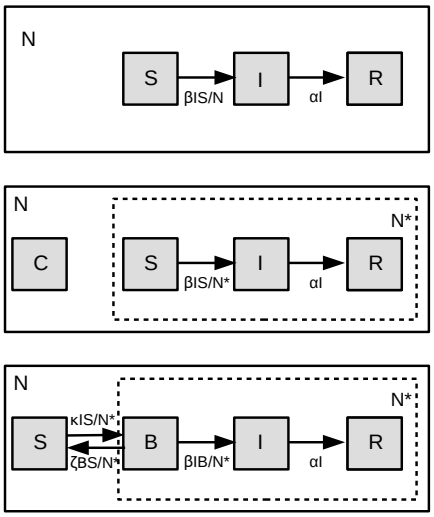

FIG. 1: Diagrammatic representation of three compartmental models, SIR, CSIR and SBIR. In SIR and CSIR three compartments interact, with the only difference in CSIR that those three compartments do not contain the entire population, since part of the population has attained cross-immunity. In the SBIR model, the susceptible part of the population is subdivided into individuals B inside the blob, and S, outside the blob.

show, by comparison with data from the Johns Hopkins University data-base [10], that the SBIR model allows to simultaneously fit the data in the increasing and decreasing phase of the epidemic without the need of adjusting the model-parameters during the epidemic (section III). The appendix contains the mathematical procedure to analytically estimate the decay exponents of the different models.

II. A CLUSTER-BASED COMPARTMENTAL MODEL

Spatially resolved epidemiological models are elegant and physically better justified than the SIR model but have the disadvantage that they are harder to analyze analytically, which makes insights on the effect of the different parameters more complicated. Indeed the complexity increases in general the descriptive capacities of a model, but decreases the insights which can be obtained.

We will propose here a new model, that does only introduce one new compartment, representing the individuals who are or have been spatially close to the infected people. Thereby our model remains based on global parameters and does not introduce the need to solve a two-dimensional diffusion problem. This simplicity allows the analytical derivation of the long-time behavior and thereby elucidates the role of local cluster-saturation on global decay-rates.

We will in this section first recall the SIR model, give

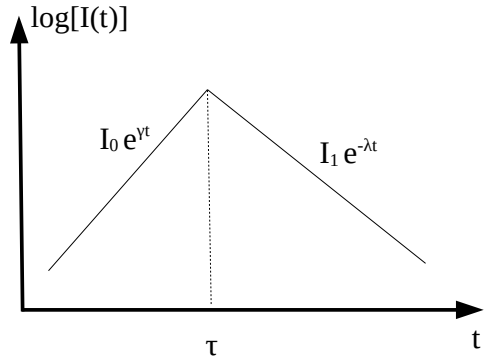

FIG. 2: Schematic representation of the evolution of the number of infected individuals in SIR and SBIR under the assumption of constant model-parameters. Time τ represents the peak-value of the number of infected.

an analytical estimate of the decay-exponent in the final phase of the epidemic, and show the influence of cross-immunity in a simple CSIR model. After that we introduce the SBIR model and discuss its physical properties.

A. The decay exponent in SIR and cross-immunity

The simplest model for macroscopic modeling of an epidemy is the Susceptible-Infected-Recovered (SIR) model [1, 11]. The model describes a population divided in three categories, Susceptible S, Infected I and Removed or Recovered R (Fig. 1, top). The total population $N = S+I+R$ is supposed constant on the timescale of the epidemic. The evolution of, and the interaction between the three compartments is given by a set of three coupled ordinary differential equations,

$$\begin{aligned} \frac{dS}{dt} &= -\beta\frac{IS}{N} \\ \frac{dI}{dt} &= \beta\frac{IS}{N} - \alpha I \\ \frac{dR}{dt} &= \alpha I. \end{aligned} \tag{1}$$

In the following it is convenient to normalize these equations by N, so that R, S, I all take values between one and zero and $S + R + I = N = 1$. Initially $R(0) = 0$, $I(0) = I_0 \ll 1$ and $S(0) = 1 - I(0) \approx 1$. The dynamics of the SIR model are characterized by an exponential growth with exponent $\gamma = \beta - \alpha$, upto a time τ where saturation of the infected is obtained, by collective, or herd immunity, obtained when $S < \alpha/\beta$. Note that in the present epidemic of SARS-CoV-2, we remain very far below such collective immunity. Long enough after this $t = \tau$, exponential decay is observed until all infected have disappeared. The behavior is sketched in Fig. 2. We show in the appendix a simple and straightforward

way to determine the approximate exponential growth and decay rate of the epidemic. This analysis, assuming continuity of two exponentials (as in Fig. 2), yields the decay-exponent

$$\lambda = \frac{\alpha\gamma}{\beta} \equiv \frac{\alpha\gamma}{\gamma+\alpha}, \tag{2}$$

which gives a direct relation between the exponential during the initial, growing phase of the epidemic, and the decaying phase. We note that an exact analytical solution of the system exists [12], but the extension of the method to more complicated systems might not be straightforward. The present approach yields less accurate but readily interpretable results, allowing direct insights in the effect of the parameters on the evolution of the epidemic.

Furthermore, the peak-value of the number of infections is given by

$$I(\tau) = \left(\frac{\gamma}{\beta}\right)^2, \tag{3}$$

and at this time τ, the rate of infection $P = \beta SI$ is close to its maximum and is given by (see appendix)

$$P(\tau) = \alpha\left(\frac{\gamma}{\beta}\right)^2. \tag{4}$$

An important question is whether cross-immunity could explain the saturation of an epidemic such as the ongoing one at the observed levels. We consider thereto a population where a part of the individuals has attained cross-immunity - the precise source of it, past contact with similar viruses or any other hidden mechanism being beyond the scope of this study. This part of the individuals is called C (Fig. 1, center). To obtain the CSIR equations, the SIR-equations are now only changed on the level of the global community size, where we replace

$$N = C+S+I+S = 1 \rightarrow N^* = S+I+R = 1-C. \tag{5}$$

The initial exponent and the value of λ are not changed by this modification for given α, β, but the peak-values of I and P are multiplied by a factor $(1-C)$ as explained in the appendix. For instance

$$P_{\text{CSIR}}(\tau) = \alpha(1-C)\left(\frac{\gamma}{\beta}\right)^2 = (1-C)P_{\text{SIR}}(\tau). \tag{6}$$

In the long-time however, the decay exponent is the same for the SIR and the SBIR model. In the SARS-CoV-2 data that we will later analyze, the infection peak is so low that the required amount of cross-immunity does not correspond to a realistic figure. Furthermore, the observed long exponential time-scale for the decay phase cannot be reproduced in a CSIR model.

B. SBIR: SIR in a Blob

We consider a cluster-based compartmental model, where a sub-ensemble of individuals $N^* < N$ belongs to a diffusing cluster interacting with infected individuals. We define the number of persons in the cluster as $N^* = B + I + R \equiv 1 - S$, where I and R have the same interpretation as before, i.e., infected and recovered/removed, respectively, and B is referred to as the blob, namely the people in the cluster who are not yet infected or recovered. These individuals can be seen as local susceptibles. The persons in S are susceptible individuals, that need first to join the blob before being possibly infected. The 4 compartments, as illustrated in Fig. 1, are now related by the following system of ordinary differential equations,

$$\frac{dS}{dt} = -\kappa\frac{SI}{N^*} + \zeta\frac{SB}{N^*} \tag{7}$$

$$\frac{dB}{dt} = \kappa\frac{SI}{N^*} - \zeta\frac{SB}{N^*} - \beta\frac{BI}{N^*} \tag{8}$$

$$\frac{dI}{dt} = \beta\frac{BI}{N^*} - \alpha I \tag{9}$$

$$\frac{dR}{dt} = \alpha I. \tag{10}$$

If the growth exponent $\gamma = \beta - \alpha$ has the same expression as in the SIR model, the final decay exponent is given by (see appendix),

$$\lambda(t) = \frac{\alpha\gamma}{\gamma + \beta\frac{B(t)}{B(\tau)}}, \tag{11}$$

which is different from the expressions for SIR and CSIR, and now depends on the temporal (physical) evolution of the blob.

Integrating the system, it is observed that, in the limit of small diffusivity, this value becomes independent of the precise value of the diffusivity and the value of $B(t) \approx B(\tau)$ after the peak of the number of infected remains approximately constant during the duration of lock-down and λ remains therefore constant in this interval.

In the other limit, of very fast diffusion, B will approach 1, and the SIR-dynamics are observed subsequently. Using in expression (11) the values $S(\tau) = \alpha/\beta$, $S_\infty = (\alpha/\beta)^2$ for $B(\tau)$ and $B(t)$, respectively (see appendix), the SIR expression (2) for the decay exponent is recovered, showing mathematical consistency. Furthermore, mathematical robustness of the formulation is ensured, since none of the quantities S, B, I, R can become negative.

C. The physics behind SBIR

Before integrating the SBIR model, it is insightful to show what the physical picture behind the model is. This will help to interpret the results and to guide the choice of

the parameters. The parameters of the model are α, β, κ and ζ. Whereas α is an intrinsic paramater characterizing the disease, β, κ and ζ depend on physical, biological and psychological influences. The β parameter, representing the infection rate is already present in the classical SIR model, and does not need further discussion here.

In order to understand the dynamics of the blob, let us consider the coupling between the S and B compartments, and first neglect the term proportional to ζ. Since $N^* = B + I + R$, we have then

$$\frac{dN^*}{dt} = \kappa \frac{SI}{B+I+R}, \tag{12}$$

so that if we have initially a very small amount of infected, $R = B \approx 0$ and $S \approx 1$, leading to

$$N^* \approx \kappa t. \tag{13}$$

This corresponds to the increase of a surface explored by a random walk, since the separation of a random walker from its initial position, $r(t) \equiv \sqrt{\langle (\boldsymbol{x}(t) - \boldsymbol{x}(0))^2 \rangle} \sim \sqrt{\kappa t}$, and the surface will be proportional to the square of this length. The interaction between the two compartments is therefore governed by a Brownian-like diffusion process. However, at longer times, the number of individuals who are infected increases rapidly, and the total time dependence of the blob-size will not necessarily follow the Brownian estimate.

We can ask how this diffusion is related to the movement of individuals. In the kinetic theory of gases, the macroscopic diffusion coefficient is related to microscopic motion by

$$\kappa_m \sim uln, \tag{14}$$

where in this expression u is the velocity magnitude of the gas-molecules, l the mean-free-path and n the number of particles. In our description, where the blob diffuses with a typical timescale κ, the value of κ can be assumed to be proportional to the number of individuals in movement n, assuming that their velocity and typical travel-distance are not considerably affected. Even though this is obviously a very rough approximation, we could use this idea to estimate the change of diffusion during lock-down using smartphone mobility data (as for instance [13, 14]). In the present investigation we will use constant model-coefficients and show that this approximation, during confinement, gives good agreement with data. The influence of non-constant coefficients is left for future investigation.

We still have the paramater ζ to discuss. The evolution equation of S can be written as

$$\frac{dS}{dt} = -\kappa \frac{SI}{N^*} \left(1 - \Gamma^{-1} \frac{B}{I}\right), \tag{15}$$

where

$$\Gamma = \kappa/\zeta. \tag{16}$$

The ratio B/I indicates how many individuals in the cluster are typically interacting with one infected. Indeed, if we set ζ to zero, there is no bound on the blob-size. A blob of one-million individuals per infected case does however not make much sense physically. The combination of the κ and ζ term will allow the system to relax to an equilibrium value Γ of the typical infection density per cluster.

We have thus given physical interpretations of the model parameters κ, ζ. In the following we will show how the SBIR model compares to realistic data for constant coefficients.

III. COMPARISON WITH DATA ON CONFIRMED INFECTIONS

In this section we compare the results of our model to recent data on the epidemic. The data of the daily confirmed new infected cases is obtained from the Johns Hopkins University data-base [10]. We have chosen to compare to several European countries where the lock-down is applied and Sweden, a country who has only applied "mild" restrictions on its population. This quantity is related to the source term in equation (9),

$$P_{\text{SBIR}} \Delta t = \beta \frac{BI}{N^*} \Delta t. \tag{17}$$

With $N^* = B + I + R$ and $\Delta t = 1$ day.

Our procedure is the following. We use for the parameter $\alpha = 0.1$ ([15, 16]) and determine in the data the time $t = 0$ where the prevalence of daily confirmed new infected cases exceeds $1 \cdot 10^{-6}$. During the early growth phase of the epidemic, the data is fitted by an exponential, thereby determining $\gamma = \beta - \alpha$. The value of the cluster diffusion κ is fixed by the height of the peak. The final parameter ζ is varied to get a best fit, limiting typically the maximum bubble-size to a concentration of maximum a few hundreds of susceptibles in the bubble per infected individual. The initial ratio $B(0)/I(0)$ is set to the value κ/ζ.

The results of the integration of the SBIR model are compared in figure 3 to the data, and the parameters are indicated on each plot. The general agreement is rather encouraging. It is observed that for all countries the value of β is of order 0.3. The value of the diffusivity varies within the subset of considered countries in the range $\kappa \in [1.3 \cdot 10^{-4}, 3.5 \cdot 10^{-4}]$ and the ζ parameter is typically 2 to 3 orders of magnitude smaller. For all countries a revival of the epidemic seems to start around day 100, which is not reproduced by the model with constant coefficients. The approximate time of this revival corresponds to the end of the lock-down period, indicated in the figures by a shaded area. We have used an objective definition for the dates of this lock-down period using mobility data from Google ([13]), given in the appendix.

Also shown in the figure for comparison are the CSIR results. We have again fitted the initial growth exponent,

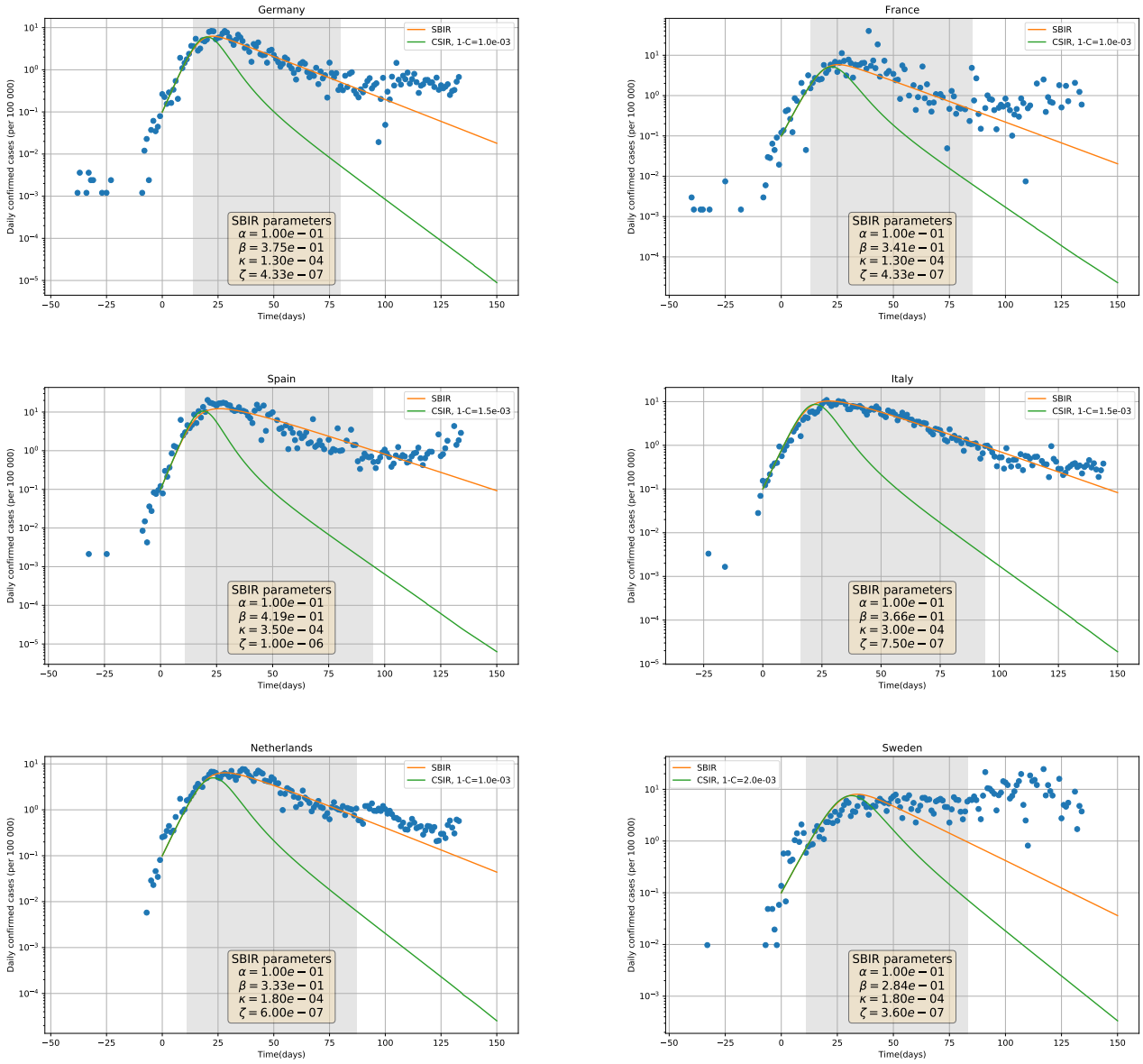

FIG. 3: Comparison of SBIR and CSIR results, with data from JHU [10] for 6 European countries. The data represent the reported daily new infections. The shaded region corresponds to the lock-down period in the different countries.

and we have adjusted the value of the cross-immunity C to reproduce the peak of infection. To obtain a correct fit we need to use a value $C \approx 0.999$, which is too large to be a realistic figure. Furthermore, the decay exponent λ gives fairly good agreement for $SBIR$, $\lambda_{\rm SBIR} \approx 0.04$, whereas the CSIR decay is closer to $\lambda_{\rm SIR} \approx 0.07$, which largely underestimates the duration of the epidemic.

We also compare fhe SBIR model to a country where lock-down restrictions were very light, Sweden. It is observed that the model does not, at all, describe the behaviour of the data in this country. One can ask what is the ingredient in the SBIR model what does make it performant to describe countries during and after lock-down, and not countries with only light restrictions. This will be discussed in the following section.

IV. DISCUSSION

We have shown that the introduction of an additional compartment in the SIR model allows to take into account the presence of clusters in the evolution of an epidemic. We have shown that the SBIR model reproduces the decay-exponent of new infections during lockdown

without the need to vary in time the model parameters over a duration exceeding 100 days.

We also show that the SBIR model in its present form reproduces countries during lock-down, but does not reproduce observations in countries long time after restrictions are weakened, or countries where restrictions on mobility were very mild (as in Sweden). We trace back the origin of this different behavior to the fact that in the SBIR model, as formulated here, all the recovered individuals R are counted in the blob-population N^*. This is plausible in lockdown countries where clusters are fixed in space, hence will saturate and suffocate when R increases. In countries where the clusters not only expand, but also relocate, the epicenter of the epidemic will move spatially and leave behind regions where a large part of the population has been touched by the epidemic, but where the disease is less active. The way in which we can model this, and thereby to take into account the dynamics of the epidemic in countries where restrictions were minor will be discussed and assessed in a future investigation.

We have deliberately chosen in the present work to consider the simplest model, SIR, and to add the effect of clustering upon this model. This allows to assess most easily the refinement. However, the nature of the present subdivision of compartments is so simple that most existing compartmental models, such as the SEIR model, can be modified in a similar manner.

Furthermore we have chosen to keep the model-constants fixed in time. This is obviously a simplification, since restrictions will have an influence on κ and β, and these quantities will vary in time. However, it is the strength of the present model that not the whole evolution depends on this adjustment, and that the saturation of the number of infected can already be described by one single set of model-constants per country. In future work this can obviously be relaxed and realistic data on mobility from mobile network providers (as used here to determine the period of lockdown) can in principle allow us to get a handle on the values of the diffusion and transmission coefficients.

Acknowledgments

The authors thank Samuel Alizon (MIGEVEC - CNRS) and Loïc Méès (LMFA - CNRS) for stimulating discussions, as well as Benjamin Pillot (UMR Espace-Dev 228) for developing the Pycovid-19 package [17] used to access data of the JHU-database and for useful advices.

[1] William Ogilvy Kermack and Anderson G McKendrick. A contribution to the mathematical theory of epidemics. *Proceedings of the royal society of london. Series A, Containing papers of a mathematical and physical character*, 115(772):700–721, 1927.

[2] Vincenzo Capasso and Gabriella Serio. A generalization of the kermack-mckendrick deterministic epidemic model. *Mathematical Biosciences*, 42(1-2):43–61, 1978.

[3] Herbert W Hethcote. The mathematics of infectious diseases. *SIAM review*, 42(4):599–653, 2000.

[4] Fred Brauer, Carlos Castillo-Chavez, and Carlos Castillo-Chavez. *Mathematical models in population biology and epidemiology*, volume 2. Springer, 2012.

[5] Nicole Mideo, Samuel Alizon, and Troy Day. Linking within-and between-host dynamics in the evolutionary epidemiology of infectious diseases. *Trends in ecology & evolution*, 23(9):511–517, 2008.

[6] James Dickson Murray, E Ann Stanley, and David L Brown. On the spatial spread of rabies among foxes. *Proceedings of the Royal society of London. Series B. Biological sciences*, 229(1255):111–150, 1986.

[7] Marcelo Kuperman and Guillermo Abramson. Small world effect in an epidemiological model. *Physical Review Letters*, 86(13):2909, 2001.

[8] Maia Martcheva. *An introduction to mathematical epidemiology*, volume 61. Springer, 2015.

[9] Hazhir Rahmandad and John Sterman. Heterogeneity and network structure in the dynamics of diffusion: Comparing agent-based and differential equation models. *Management Science*, 54(5):998–1014, 2008.

[10] Ensheng Dong, Hongru Du, and Lauren Gardner. An interactive web-based dashboard to track covid-19 in real time. *The Lancet infectious diseases*, 20(5):533–534, 2020.

[11] Odo Diekmann, Johan Andre Peter Heesterbeek, and Johan AJ Metz. The legacy of kermack and mckendrick. *Publications of the Newton Institute*, 5:95–115, 1995.

[12] Tiberiu Harko, Francisco SN Lobo, and MK Mak. Exact analytical solutions of the susceptible-infected-recovered (sir) epidemic model and of the sir model with equal death and birth rates. *Applied Mathematics and Computation*, 236:184–194, 2014.

[13] Covid19 mobility reports google. `https://www.google.com/covid19/mobility`. Accessed: 2020-07-03.

[14] Covid19 mobility trends apple maps. `https://www.apple.com/covid19/mobility`. Accessed: 2020-07-03.

[15] Huaiyu Tian, Yonghong Liu, Yidan Li, Chieh-Hsi Wu, Bin Chen, Moritz UG Kraemer, Bingying Li, Jun Cai, Bo Xu, Qiqi Yang, et al. An investigation of transmission control measures during the first 50 days of the covid-19 epidemic in china. *Science*, 368(6491):638–642, 2020.

[16] Yinon M Bar-On, Ron Sender, Avi I Flamholz, Rob Phillips, and Ron Milo. A quantitative compendium of covid-19 epidemiology. *arXiv preprint arXiv:2006.01283*, 2020.

[17] Benjamin Pillot and Louis Gostiaux. Pycovid-19 python library by b. pillot and l. gostiaux. `https://framagit.org/benjaminpillot/covid-19`. Accessed: 2020-07-03.

Appendix: approximate analytical determination of decay exponents in compartmental models

A. Analytical determination of the decay exponent in SIR

The decay exponent in the SIR model can be approximated analytically. We define $t = \tau$ the time where the number of infected I peaks ($dI/dt = 0$). We observe exponential increase and decay before and after this time, respectively (see Fig. 2),

$$I(t \ll \tau) = I_0 \exp(\gamma t), \quad I(t \gg \tau) = I_1 \exp(-\lambda t). \quad (18)$$

For short times $S \approx 1$. For very long times, $I \ll R, S$. Therefore

$$\begin{aligned} \gamma &= \beta - \alpha, & (19)\\ -\lambda &= \beta(S_\infty) - \alpha & (20)\\ &= \gamma - \beta R_\infty. & (21) \end{aligned}$$

In order to determine λ, we need therefore the total number of recovered, R_∞, given by

$$R_\infty = \alpha \int_0^\infty I(t)dt. \quad (22)$$

Since we assume exponentials increasing for short time and decreasing for long times, respectively, continuity at $t = \tau$ allows to write,

$$\begin{aligned} R_\infty &= \alpha \int_0^\tau I(t)dt + \alpha \int_\tau^\infty I(t)dt & (23)\\ &= \alpha \left(\frac{1}{\gamma} + \frac{1}{\lambda}\right) I(\tau), & (24) \end{aligned}$$

which expresses R_∞ as a function of a new unknown, $I(\tau)$, the peak-value of I. Considering the I-equation,

$$d_t I = (S\beta - \alpha)\, I, \quad (25)$$

the term in brackets vanishes for $S = \alpha/\beta$. We know that $S = 1 - I - R$, we also have that in the initial exponential phase

$$R = \frac{\alpha}{\gamma} I \quad (26)$$

and therefore

$$\begin{aligned} \alpha/\beta &= 1 - (1 + \alpha/\gamma) I(\tau) & (27)\\ &= 1 - (\beta/\gamma) I(\tau). & (28) \end{aligned}$$

so that

$$I(\tau) = \left(\frac{\gamma}{\beta}\right)^2 \quad (29)$$

Which yields an expression for $I(\tau)$. We have therefore the relations (21), (24), (28) for the unknown quantities, I_τ, R_∞ and λ. Solving this system yields

$$\lambda = \frac{\alpha\gamma}{\beta} = \frac{\alpha(\beta - \alpha)}{\beta}. \quad (30)$$

Note that for typical values, for instance $\alpha = 0.2$; $\beta = 0.4$, this yields $\lambda = 0.1$. Numerical integration yields $\lambda = 0.119$. This error of 20% is due to the assumptions of the two exponentials near the peak, where the rounding of the integrals significantly contributes to the error.

The quantity that we will consider in the comparison with data is the daily confirmed new infected P, which is associated with the source term in the I-equation,

$$P = \beta S I \Delta t, \quad (31)$$

where in our system, where the time-unity is days, $\Delta t = 1$.

Interesting relations, when substituting this value for λ in the equations are

$$\begin{aligned} I(\tau) &= \left(\frac{\gamma}{\beta}\right)^2, \quad P(\tau) = \alpha \left(\frac{\gamma}{\beta}\right)^2 & (32)\\ S(\tau) &= \frac{\alpha}{\beta}, \quad R(\tau) = \frac{\gamma}{\beta}\left(1 - \frac{\gamma}{\beta}\right), & (33)\\ R_\infty &= 1 - \frac{\alpha^2}{\beta^2}, \quad S_\infty = \frac{\alpha^2}{\beta^2}. & (34) \end{aligned}$$

B. Exponent in SIR with Cross immunity (CSIR)

Let us now consider the case of a partially immune population,

$$1 = C + S + I + R, \quad (35)$$

where $I(0)/S(0)$ and $R(0)/S(0)$ are small (as in the previous case), so that $S(0) \approx 1 - C$. The I-equation reads

$$\frac{dI}{dt} = \beta \frac{IS}{1 - C} - \alpha I. \quad (36)$$

For short times, we have thus, since $S \approx 1 - C$ that,

$$\gamma = \beta - \alpha, \quad (37)$$

as for SIR. The growth of I halts at time τ when $dI/dt = 0$, so that we find for $S(\tau)$

$$S(\tau) = (1 - C)\frac{\alpha}{\beta}. \quad (38)$$

We find then for the different quantities, following the same reasoning as in the previous section,

$$I(\tau) = (1 - C)\left(\frac{\gamma}{\beta}\right)^2, \quad P(\tau) = \alpha(1 - C)\left(\frac{\gamma}{\beta}\right)^2 \quad (39)$$

and for the exponential decay-rate,

$$\lambda = \frac{\alpha\gamma}{\beta}, \quad (40)$$

as for SIR.

What we learn from this is that, cross-immunity or not, if we measure γ, initially, λ is not influenced for a given α. Only the height of the peak of the number of infected I, and of the daily confirmed cases P will be multiplied by $1 - C$.

C. Exponent in SBIR

Let us now consider SBIR. The I equation of SBIR reads,

$$\frac{dI}{dt} = \left(\beta \frac{B}{1-S} - \alpha\right) I. \tag{41}$$

with $1 - S = B + I + R$. We will follow the same steps as for SIR and again we assume exponentials. The exponents are now

$$\gamma = \beta - \alpha, \tag{42}$$

$$-\lambda(t) = \beta \frac{B(t)}{B(t) + R_\infty} - \alpha. \tag{43}$$

We see thus that no pure exponential is observed. However, we have observed that the temporal evolution of B is slow for the relevant parameters so that the exponential timescale is close to constant. Let us; as in SIR, determine R_∞ by integrating the infection curve over all time,

$$R_\infty = \alpha \int_0^\tau I(t)dt + \alpha \int_\tau^\infty I(t)dt \tag{44}$$

$$= \alpha \left(\frac{1}{\gamma} + \frac{1}{\lambda}\right) I(\tau), \tag{45}$$

exactly as for SIR. Again we will determine the peak-value $I(\tau)$ of the infection curve, yielding now

$$\alpha/\beta = \frac{B(\tau)}{B(\tau) + I(\tau) + R(\tau)} \tag{46}$$

$$= \frac{B(\tau)}{B(\tau) + \frac{\beta}{\gamma} I(\tau)} \tag{47}$$

with an additional unknown $B(\tau)$, related to $I(\tau)$, by

$$B(\tau) = I(\tau) \frac{\beta\alpha}{\gamma^2} \tag{48}$$

Determining λ from these expressions, we find

$$\lambda = \frac{\alpha}{1 + \frac{\beta}{\gamma} \frac{B(t)}{B(\tau)}}. \tag{49}$$

We have thus a closed function for λ if we find an expression for $B(t)/B(\tau)$. From the integration of the system, we have seen that for the physically relevant cases $B(t)/B(\tau) \approx 1$, which yields for the specific case $\beta = 3\alpha$, $\lambda = 2\alpha/5$.

Use of Google mobility-data to determine lock-down data

We use the mobility data provided by Google [13] to determine the dates of the lock-down in the different countries. Fig. 4 shows the variations of mobility compared to

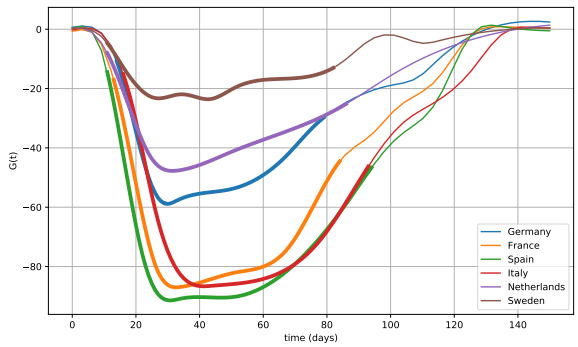

FIG. 4: Estimation of the lock-down dates from Google mobility reports [13].

a reference-value measured mid-january for the six countries considered in this work.

We have smoothened the data to get rid of high-frequency variations. We call the smoothened variable $\mathbf{G}(t)$. The general trend shows that during the epidemic the mobility drops to a value depending on the restrictions in the different countries. An approximate plateau value is observed. We take for each country the minimum value of this plateau as the reference mobility-level during lock-down, indicated by $\mathbf{G}_0$. The beginning of lock-down is then determined for the time when for the first time $\mathbf{G}(t) < 1.15\ \mathbf{G}_0$ and the end, the first later date where $\mathbf{G}(t) > 1.5\ \mathbf{G}_0$. These begin and end dates are used to indicate the lock-down periods in the different countries in Fig. 3.